Int. J. Heat Mass Transfer. Vol. 24, No. 6, pp. 1051–1057, 1981
Printed in Great Britain

0017-9310/81/061051-07 $02.00/0
Pergamon Press Ltd.

A TWO WAVELENGTH HOLOGRAPHIC TECHNIQUE FOR THE STUDY OF TWO-DIMENSIONAL THERMAL BOUNDARY LAYERS

P. J. WALKLATE
Engineering Sciences Division, A.E.R.E. Harwell, Oxon, U.K.

(*Received* 17 *January* 1980 *and in revised form* 30 *December* 1980)

Abstract—A two wavelength holographic interferometer is used to obtain heat transfer coefficient in a turbulent two-dimensional thermal boundary layer. This type of flow problem imposes some restrictions on the interpretation of interferometric data particularly in regions of the flow where large turbulence eddies exist. However, in the region of the flow near a heated wall, optical measurements of both temperature and temperature gradient are obtained by utilising different wavefront reconstruction optics. The heat transfer coefficients are inferred from this data by a statistical curve fitting procedure which utilizes redundant data to minimize any dependence on individual measurement error. The resulting curves are used to perform the extrapolations to obtain wall values.

NOMENCLATURE

C_f, friction factor $2\tau_w/(\rho U_B^2)$;
C_p, specific heat;
D_e, equivalent duct diameter $4 \times$ cross-sectional area/wetted perimeter;
f, focal length of Schlieren mirror in Fig. 2;
F, grating frequency of the hologram;
K, Gladstone–Dale constant;
l, optical path length across the working section heater;
n, refractive index;
n_e, refractive index of the extraordinary ray within the Wollaston prism;
n_o, refractive index of the ordinary ray within the Wollaston prism;
Nu, Nusselt number $D_e(\mathrm{d}T/\mathrm{d}y)|_{y=0}/(T_w - T_B)$;
Pr, Prandtl number;
q_w, wall heat flux;
Re, Reynolds number $D_e U_B/v$;
S, fringe order;
T, absolute temperature;
T_B, bulk temperature;
T_r, reference temperature;
T_w, wall temperature;
T^+, nondimensional temperature $(T_w - T)\rho C_p \sqrt{(\tau_w/\rho)}/q_w$;
U_B, bulk velocity;
x, coordinate of undisturbed ray path;
y, wall normal displacement;
y^+, nondimensional wall normal displacement $y\sqrt{(\tau_w/\rho)}/v$.

Greek symbols

α, wedge angle of Wollaston prism;
δ, angle between the heater surface and a line perpendicular to the background fringes on the Schlieren interferogram;
λ, wavelength of light;
θ, angle between object and reference beam in the holographic interferometer;
v, kinetic viscosity;
ρ, density;
ρ_r, reference density;
τ_w, wall shear stress;
ϕ, ray path within the working fluid.

INTRODUCTION

OPTICAL interferometry provides the engineer with an extremely versatile tool for making quantitative measurements of thermal diffusion phenomena. For many years the most common optical apparatus in use in the engineering laboratory has been the Mach–Zehnder interferometer. However, advances in holographic recording techniques, since the commercial availability of suitable lasers and the pioneering work of Gabor [1] and Leith and Upatnieks [2], have led to the development of an extremely versatile family of holographic interferometers.

The purpose of this work is to test the suitability of a two wavelength holographic interferometer for studying turbulent two-dimensional thermal boundary layer problems. Turbulence imposes some limitations on the direct interpretation of interferometric data because the measured spacial integrals of temperature are time dependent in regions of the flow where large turbulence eddies exist. This is not an insurmountable problem for holographic interferometry if a good panoramic view of the flow is possible [3]. However, the data reduction problems associated with the multidirectional holographic interferometer would make the experiments prohibitively expensive. More immediate attention has therefore been focused on the near wall region of the flow. In this region turbulence eddies are small compared with the total disturbed optical path of the interferometer. Therefore, the line integral measurement on a plane parallel with the wall becomes independent of time. Moreover, in a two-dimensional mean flow these line integrals of temperature approach the values of the time integrals. This approximation was previously invoked by Kulacki and Goldstein [4] to determine details of turbulent thermal convection from a single interferometric record.

By utilizing Schlieren techniques to inspect reconstructed wavefronts from holographic recordings it is possible to record the temperature difference field as well as the temperature field by photographic means. This versatility makes the technique very useful for studying thermal diffusion around solid bodies with complex shapes (in one plane) and with complex heat flux distributions.

GENERAL PRINCIPLES OF HOLOGRAPHIC RECORDING

A holographic recording is made by exposing a light sensitive recording material to the interference pattern generated by two mutually coherent beams of light (object and reference beams). When developed the recorded pattern (hologram) is illuminated with the reference beam only. In this process, known as wavefront reconstruction, the hologram acts like a complex grating and diffracts some of the light to reproduce the phase and amplitude detail of the original object beam. By combining two such reconstructed wavefronts an interference pattern can readily be observed. This interference pattern is directly related to the phase change of the object beam between exposures of the hologram. In the experiment reported here, changes in the phase of the object beam are induced by changing the thermal boundary condition in an incompressible duct flow. The physical laws which relate gas temperature changes along a ray path to its interferometric phase record are well known and are discussed in detail by Hauf and Grigull [5].

INTERFEROMETER DESIGN CONSIDERATIONS

By using the holographic recording technique, optical interferometry can be achieved with relatively low grade optical components (e.g. windows, mirrors, etc.) and even with diffuse object illumination [3, 6]. However, the interpretation of interferograms with diffuse object illumination is often more complicated than those with collimated object illumination, particularly near irregular solid surfaces. Also, the resolution limit of a diffuse object interferogram is significantly lower than that achieved with collimated object illumination, because of the speckle pattern associated with coherent light on a diffuse surface [7]. Another advantage of a collimated object beam is that it can be easily inspected in a Schlieren system. However, in order to gain useful quantifiable information this way the optical surfaces in the object beam must be of normal Schlieren quality. It must also be possible to separate the wavefront reconstructions. Mayinger and Panknin [8] used two separate reference beams to produce separable reconstructed wavefronts from a single plate. Alternatively, Havener [9] used separate holographic plates to record wavefronts from a heated and unheated scene. These plates were used individually to reconstruct single wavefronts or combined by using a precision adjustable plate holder to form holographic interferograms. The main disadvantage of this procedure is the amount of time required in setting up the precision plate holder. The approach adopted here is similar to Mayinger and Panknin [8]. However, in this case the two separate holographic grating frequencies are obtained by using two wavelengths of laser light to record the heated wavefront. The main advantage of this over the geometrically separated reference beams used by Mayinger and Panknin is that it minimizes the amount of optical hardware required to build the interferometer.

EXPERIMENTAL TECHNIQUE

Figure 1 shows the optical arrangement used for recording and reconstructing optical wavefronts from

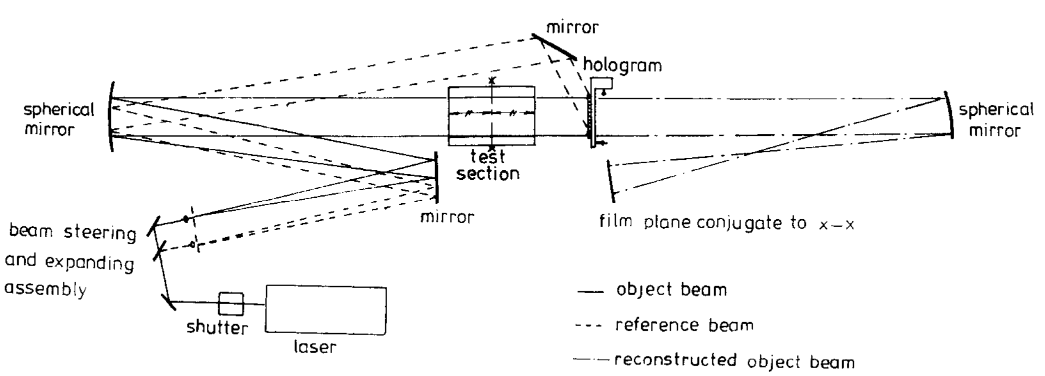

FIG. 1. Arrangement for recording and reconstructing optical wavefronts.

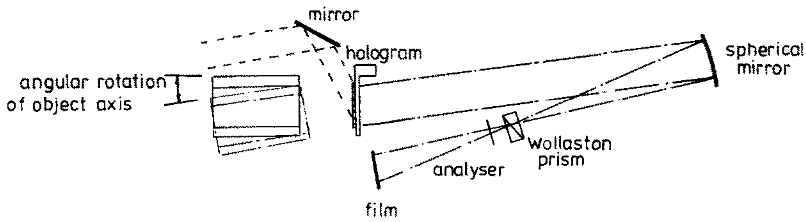

FIG. 2. Arrangement of reconstruction optics with Schlieren interferometer.

the wind tunnel working section. A recording of the unheated working section was made with a single wavelength of laser light ($\lambda_1 = 0.5145\,\mu$m from an argon ion laser). The wind tunnel heater was switched on and allowed to attain a steady-state condition. Two more recordings were then made on the same photographic plate; one recording in wavelength λ_1 and the other in $\lambda_2 = 0.488\,\mu$m.

The spacial frequency of a hologram is given by

$$F = \frac{\sin\theta}{\lambda} \tag{1}$$

(typical $\theta = 60°$).

Therefore, the holographic interferogram, recorded with λ_1, has a spacial frequency of 1683 lines/mm and the other holographic recording of the heated wavefront, recorded with λ_2, has a spacial frequency of 1774 lines/mm. The photographic emulsion 10E56 made by Agfa–Gevaert was found to be a suitable recording material combining a good compromise between speed and resolution. The emulsions were exposed with a reference to object beam intensity ratio of $\simeq 7:1$ and developed to a mean density of $\simeq 0.7$ in Neofin Blue concentrate (Tetanal). Finally, the plates were fixed in Agfa–Gevaert G334 fixer for 3 min then washed in running water for at least 15 min before they were allowed to dry.

Wavefront reconstruction was obtained by illuminating the developed plates with a single wavelength reference beam. The reconstructed wavefronts which form the holographic interferogram are separated by a small angle $\Delta\theta$ from the reconstructed wavefront of the heated working section recorded in λ_2 where

$$\Delta\theta = \sin^{-1}\left(\frac{\lambda_1 \sin\theta}{\lambda_2}\right) - \theta \tag{2}$$

for a reference beam of wavelength λ_1. Therefore, $\Delta\theta = 5.9°$. This was more than sufficient to eliminate any overlapping of the wavefronts at the image plane. The reconstruction optics used to produce the holographic and Schlieren interferograms are shown in Figs. 1 and 2, respectively.

DATA REDUCTION

Writing the equation of interferometry given by Hauf and Grigull [5] in terms of temperature for an incompressible two dimensional boundary layer

$$T_i = T_r\left(1 - \frac{S\lambda C_{1i}}{K\rho_r l}\right)^{-1} \tag{3}$$

where the subscript r indicates fluid properties evaluated at a reference temperature and C_{1i} is a correction term which accounts for the phase difference between the measured ray path and the ideal ray path which is parallel with the wall. The correction is given by

$$C_{1i} = l\left(T_{\phi=0}\int_{\phi}\frac{d\phi}{T(\phi)}\right)^{-1}\Bigg|_{i-1} \tag{4}$$

where the subscript $i-1$ indicates that the temperature field is given by its previous estimate.

Merzkirch [10] has shown that the density difference normal to the direction of the background fringes can be measured directly from a Schlieren interferogram. Therefore

$$\Delta\rho = \left(\frac{\Delta S}{S}\right)\frac{\lambda}{lK}. \tag{5}$$

Writing equation (5) as a temperature difference it can be shown that

$$\Delta T_i = C_{2i}\frac{\lambda T_r}{lK\rho_r}\left(\frac{\Delta S}{S}\right) \tag{6}$$

where

$$C_{2i} = \frac{T_{i-1}|_{y+\Delta y/2}\, T_{i-1}|_{y-\Delta y/2}}{T_r^2}$$

and

$$\Delta y = \frac{2f(n_o - n_e)\tan\alpha}{\sin\delta}.$$

This is the difference form of equation (1) given by Sernas and Fletcher [11].

To minimize any dependence on individual measurement errors, equations (3) and (6) were used as input to a series expansion for $T(y)$ made up of 5 piecewise smooth third-order polynomials with continuous first- and second-order derivatives. The resulting set of linear algebraic equations were solved as an overdetermined problem for a least squares residual error, in accordance with Wilkinson and Reinsch [12]. Small corrections for the nonlinearities in equations

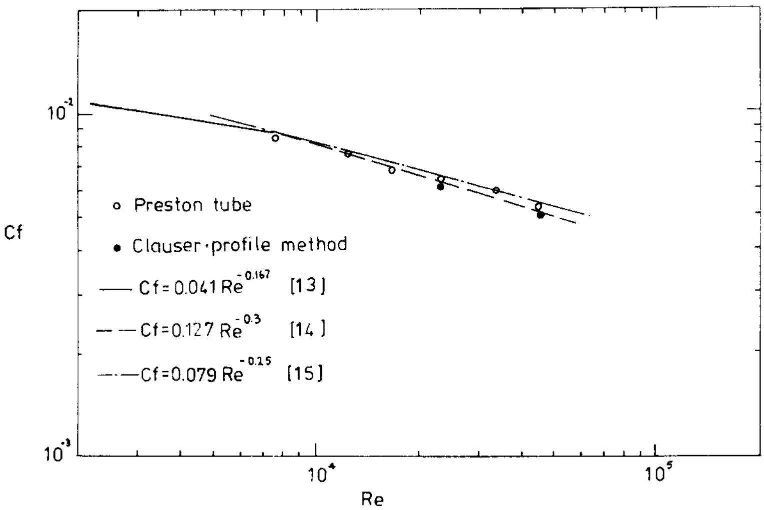

FIG. 3. Friction factor results for a rectangular duct.

(3) and (6) were included by iteration of the whole procedure. Initial estimates of C_{i1} and C_{i2} were set at unity with subsequent estimates of C_{i1} based on numerical estimates of the ray path from refraction theory.

WIND TUNNEL DETAILS

The measurements presented were obtained at a position 27 hydraulic diameters from the inlet with electrical resistance heating commencing after 20 hydraulic diameters. The working section was rectangular with an aspect ratio of 4:1 and a hydraulic diameter of 0.122 m. To ensure good optical access for the interferometer, Schlieren quality glass windows were fitted in both sides of the working section.

DISCUSSION OF EXPERIMENTAL RESULTS

Preliminary friction factor measurements were made with a Preston tube and these results, which are presented in Fig. 3, show good agreement with empirical laws for rectangular ducts [13–15]. At the higher Reynolds number flows the Preston tube method was checked against the Clauser profile method for determining friction factors. These results are also shown in Fig. 3 and again the agreement is well within the limits of the measurement accuracy.

Typical examples of holographic and Schlieren interferograms are shown in Figs. 4 and 5, respectively. Data reduction of the photographic information was performed by eye with an optical comparitor. Fringe displacement due to refraction was corrected, to a first

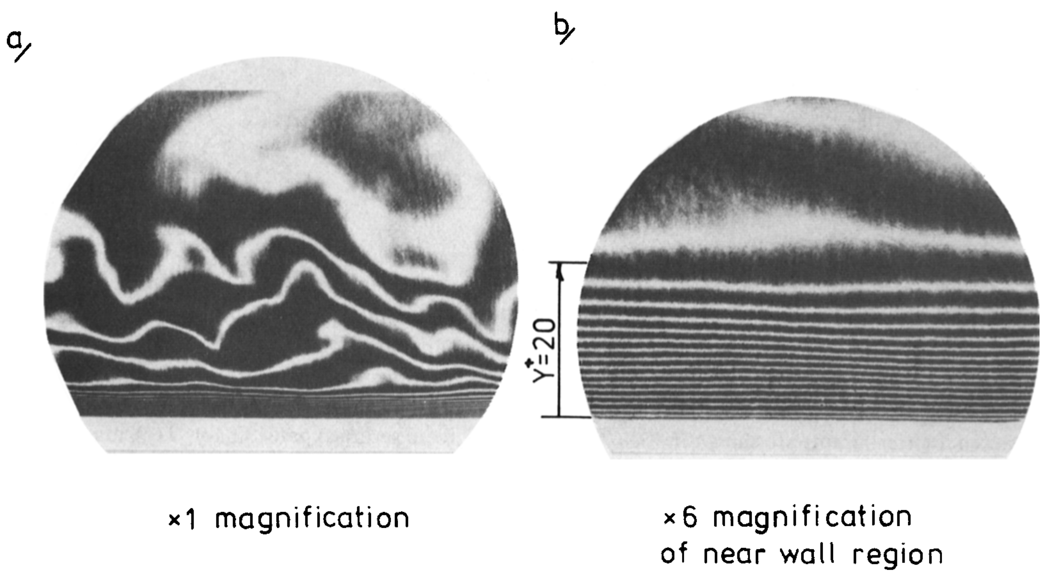

FIG. 4. Holographic interferograms of a heated rectangular duct at Re = 5400.

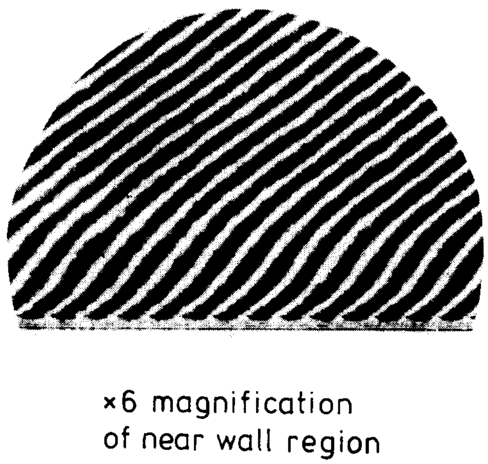

FIG. 5. Schlieren interferogram of a heated rectangular duct at $Re = 5400$.

order approximation, by focusing on the working section centre plane. This was calculated to optimize the displacement correction for the light rays refracted by the near wall region where $\mathrm{d}T/\mathrm{d}y$ is approximately constant, and assuming an ideal two-dimensional mean flow. The displacement correction for the light rays further away from the wall are less well optimized, however, the corresponding displacement effects are also smaller. The interpretation and statistical curve fitting of the experimental data was performed by a computer program based on the equations outlined in this report. Figure 6 shows a comparison between bulk heat transfer coefficient determined by this interferometric method and those determined by an energy balance. These results are reasonably consistent with the empirical relationship

$$Nu = 0.023\, Re^{0.8}\, Pr^{0.4} \tag{7}$$

over the experimental range $0.5 \times 10^3 < Re < 4 \times 10^4$. However, the interferometric results are consistently lower than the energy balance results by as much as 17% at $Re = 4 \times 10^4$; although the agreement is much better than this at lower Reynolds numbers. This error may be attributed to a small misalignment of the heater wall which appears much enhanced in the thinner thermal boundary layers at higher Reynolds numbers. A comparison between the interferometric data and the 'universal' temperature profile [16] is shown in Fig. 7. Good agreement between interferometric measurements and accepted theory is demonstrated in the near wall flow region $y^+ < 20$, and justifies confidence in the extrapolation procedure. Hinze [17] includes some measurements that show turbulence intensities reach a peak within this region of a fully developed boundary layer. Despite this, interferometric spacial averages exhibit little or no time dependence [Fig. 4(b)] and are reasonably consistent with time averaged values of temperature.

The overall effects of refraction produce the upper working limits for mass flow and heat flux for a given geometry and working fluid. It is useful to relate these parameters to one refraction parameter, and this can be achieved by considering the maximum ray displacement in a thermal boundary layer. From refraction theory

$$\frac{\mathrm{d}^2 y}{\mathrm{d}x^2} = \left[\frac{-K\rho r}{(T/T_r + K\rho r)T}\right]\frac{\mathrm{d}T}{\mathrm{d}y}. \tag{8}$$

For the flow region near the heated wall

$$\frac{\mathrm{d}T}{\mathrm{d}y} = \left.\frac{\mathrm{d}T}{\mathrm{d}y}\right|_{y=0}.$$

Also, for the range of experiments $\Delta T \ll T_r$. Using these simplifications, equation (8) can be integrated with ease to obtain the maximum wall-normal dis-

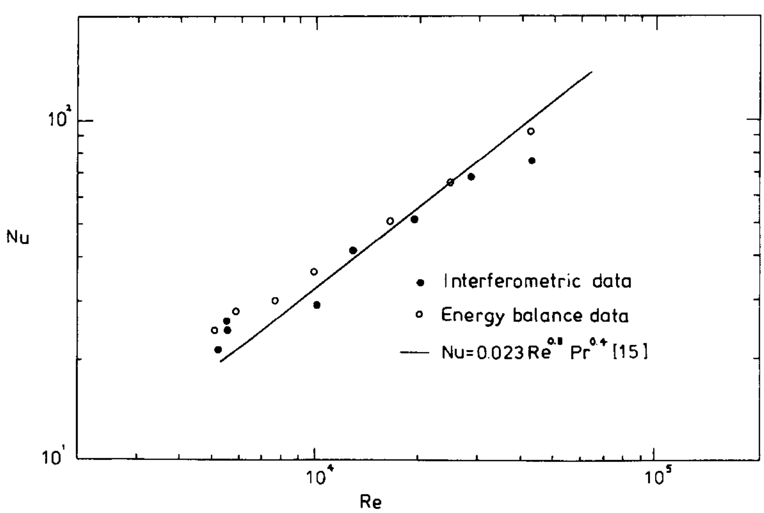

FIG. 6. Heat transfer results for a rectangular duct.

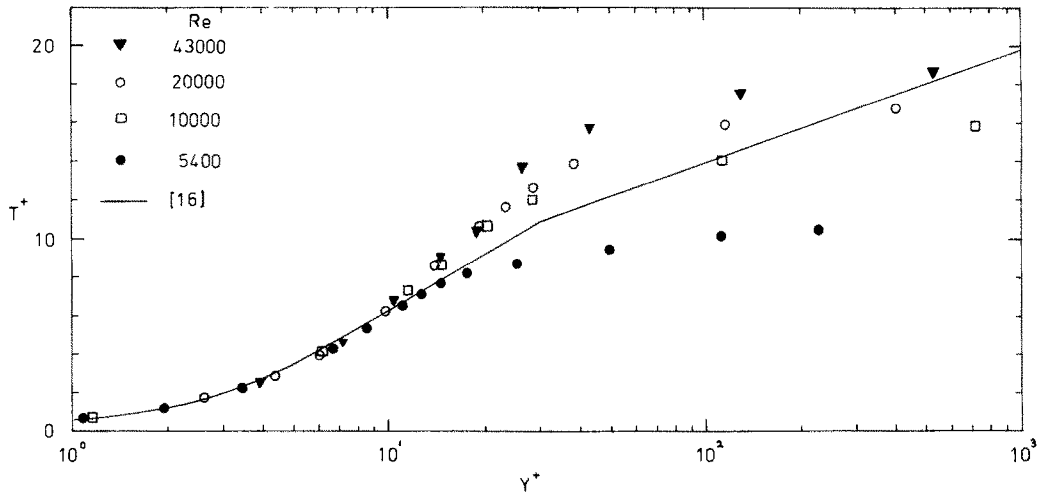

FIG. 7. Temperature profiles for a rectangular duct.

placement, which is expressed as a Reynolds number as follows

$$\Delta y^+ = \frac{\Delta y\sqrt{(\tau\omega/\rho)}}{\nu} = \frac{K\rho r}{(1+K\rho r)} \times \frac{\Delta T}{T} Nu Re\sqrt{(C_f/2)}(x/D_e)^2 \tfrac{1}{2} \quad (9)$$

where $\Delta T = T_w - T_B$.

If we make use of the expression $C_f = 0.127Re^{-0.3}$, and equation (7), to eliminate C_f and Nu from equation (9), we obtain the following equation for a turbulent duct flow with smooth boundaries

$$\Delta y^+ = 0.0029\left(\frac{K\rho r}{1+K\rho r}\right)Pr^{0.4}\frac{\Delta T}{T}\left(\frac{x}{De}\right)^2 Re^{1.65}. \quad (10)$$

The maximum acceptable value for Δy^+ can therefore be estimated with $Re = 3 \times 10^4$ and using properties of air at 1 atm and $T = 310$ K: $K\rho r = 2.576 \times 10^{-4}$, $Pr = 0.7$, $\Delta T = 15$ K and $X/D_e = 2.5$, then $\Delta y^+ = 4.8$. For $Re > 30000$ the general agreement between experimental data and theory shown in Fig. 6, deteriorates. However, the Reynolds number range could be further extended by using a finite background fringe system [5]. This increases the resolution of the temperature field by improving the resolutions of the fringe system. For example ΔT could be reduced by an order of magnitude and therefore the technique could be extended to $Re = 10^5$. Also given that $\Delta y^+ = 4.8$ is the maximum working value for the interferometric technique, equation (9) could be used to determine the maximum measurable Nusselt number for a given ΔT, Re and C_f in a new two-dimensional boundary layer configuration.

CONCLUSIONS

The two wavelength holographic technique coupled with a statistical data curve fitting technique has been demonstrated to give good estimates of heat transfer coefficients in a turbulent two-dimensional mean flow over a limited range of Reynolds numbers $5 \times 10^3 < Re < 4.3 \times 10^4$ for a duct of aspect ratio 4:1.

The holographic technique gives a photographic record of both the line integral of the temperature and the temperature difference fields at a single instance of time. However, it has been demonstrated that in a turbulent two-dimensional mean flow the line integrals, determined by the interferometric technique, are in good agreement with the time integrals in the flow region near the heated wall ($y^+ < 20$). Thus heat transfer coefficients can be deduced from a holographic record of a single event.

A refraction displacement Reynolds number, given by equation (9), has been used to define the upper limit of applicability of the interferometric technique and this was found to be $\Delta y^+ = 5$.

Optical experiments can easily be performed on holographically reconstructed wavefronts. Thus obviating any necessity to re-run the experimental flow rig. This has advantages on large scale flow rigs where it may be very costly to repeat heat transfer tests.

The combination of holographic and Schlieren interferometric information can reduce any ambiguity in the interpretation of data from less well-known flow problems. Thus the technique could be directly applied to two-dimensional mean flows with more complex wall geometries (e.g. flow over rib roughened surfaces).

Acknowledgements—The experimental work described above was done in the Department of Engineering Science at Oxford University and was financially supported by the Engineering Sciences Division, A.E.R.E. Harwell.

REFERENCES

1. D. Gabor, Microscopy by reconstructed wavefronts, *Proc. R. Soc.* **A197**, 454–487 (1949).

2. E. N. Leith and J. Upatnieks, Reconstructed wavefronts and communication theory, *J. Opt. Soc. Am.* **52**, 1123–1130 (1962).
3. D. W. Sweeney and C. M. Vest, Measurement of three-dimensional temperature fields above heated surfaces by holographic interferometry, *Int. J. Heat Mass Transfer* **17**, 1443–1453 (1974).
4. F. A. Kulacki and R. J. Goldstein, Eddy heat transport in thermal convection with volumetric energy sources, *5th Int. Heat Transfer Conference* (Tokyo) **3**, 64–68 (1970).
5. W. H. Hauf and U. Grigull, Optical methods in heat transfer, *Adv. Heat Transfer* **6**, 133–366 (1970).
6. J. W. C. Gates, Holography with scatter plate, *J. Sci. Instrum. (J. Phys. F)* Ser. 2, **1**, 989–994 (1968).
7. F. C. Jahoda and R. E. Siemon, Holographic interferometry cookbook, Los Alamos report no. La-5058-MS (1972).
8. F. Mayinger and W. Panknin, Holography in heat and mass transfer, *5th Int. Heat Transfer Conference* (Tokyo) **5**, 28–43 (1974).
9. A. G. Havener, Detection of boundary layer transition using holography, *AIAA* **15**, 592–593 (1977).
10. W. F. Merzkirch, A simple Schlieren interferometer system, *AIAA* **3**, 1974–1976 (1965).
11. V. Sernas and L. S. Fletcher, A Schlieren interferometer method for heat transfer studies, *Trans. ASME, J. Heat Transfer* **92**, 202–204 (1970).
12. J. M. Wilkinson and C. Reinsch, Handbook of Automatic Computation Linear Algebra, p. 12. Springer-Verlag, Berlin (1971).
13. V. C. Patel and M. R. Head, Some observations on skin friction and velocity profiles in fully-developed pipe and channel flows, *J. Fluid Mech.* **38**, 181–201 (1969).
14. G. S. Beaver, E. M. Sparrow and J. R. Lloyd, Low Reynolds number turbulent flow in large aspect ratio rectangular ducts, *Trans. ASME J. Basis Engineering* **93**, 296–299 (1971).
15. J. C. Han, L. R. Glicksman and W. M. Rohsenow, An investigation of heat and friction for rib roughened surfaces, *Int. J. Heat Mass Transfer* **21**, 1143–1156 (1978).
16. E. R. G. Eckert and R. M. Drake, *Heat and Mass Transfer*, McGraw-Hill, New York (1959).
17. J. O. Hinze, *Turbulence* p. 656, 2nd edn., New York (1975).

UNE TECHNIQUE HOLOGRAPHIQUE A DEUX LONGUEURS D'ONDE POUR L'ETUDE DES COUCHES LIMITES THERMIQUES BIDIMENSIONNELLES

Résumé—On utilise un interféromètre holographique à deux longueurs d'onde pour obtenir le coefficient de transfert thermique, turbulente et bidimensionnelle. Ce type d'écoulement impose quelques restrictions sur l'interprétation des données interférométriques, en particulier dans les régions de l'écoulement où existent de grands tourbillons. Néanmoins dans la région proche de la paroi chaude, on obtient à la fois des mesures optiques de la température et du gradient de température. Les coefficients de transfert thermique sont déduits des mesures par une procédure basée sur une courbe statistique et qui utilise les données redondantes pour minimiser les erreurs de mesures individuelles. Les courbes résultantes sont utilisées pour faire les extrapolations et obtenir les valeurs à la paroi.

EINE HOLOGRAFIETECHNIK MIT ZWEI WELLENLÄNGEN ZUR UNTERSUCHUNG VON ZWEIDIMENSIONALEN THERMISCHEN GRENZSCHICHTEN

Zusammenfassung—Ein holografisches Interferometer mit zwei Wellenlängen wird dazu benutzt, den Wärmeübergangskoeffizienten in einer turbulenten zweidimensionalen thermischen Grenzschicht zu erfassen. Diese Art von Strömungsproblem bringt bei der Interpretation interferometrischer Daten einige Beschränkungen mit sich, besonders für die Strömungsgebiete wo große Wirbelturbulenzen auftreten. Jedoch werden im Strömungsgebiet nahe an einer beheizten Wand optische Messungen der Temperatur und des Temperaturgradienten durch die Anwendung unterschiedlicher Optiken zur Rekonstruktion der Wellenfronten erhalten. Die Wärmeübergangskoeffizienten werden aus diesen Daten mit Hilfe einer statistischen Kurvenanpassungsmethode gewonnen, die die große Datenmenge dazu benutzt, die Abhängigkeit vom individuellen Meßfehler zu minimieren. Die sich daraus ergebenden Kurven werden zur Extrapolation auf die Wandwerte verwendet.

ДВУХВОЛНОВОЙ ЛОГОГРАФИЧЕСКИЙ МЕТОД ИССЛЕДОВАНИЯ ДВУХМЕРНЫХ ТЕПЛОВЫХ ПОГРАНИЧНЫХ СЛОЕВ

Аннотация — С помощью двухволнового логографического интерферометра определено значение коэффициента теплообмена в турбулентном двухмерном тепловом пограничном слое. Проблема течения такого типа накладывает некоторые ограничения на расшифровку интерферометрических данных особенно в областях течения, где существуют большие турбулентные вихри. Однако в области нагретой стенки как температура, так и температурный градиент могут быть измерены с помощью различных оптических устройств, в которых возможно восстановление волнового фронта. По измеренным значениям определяются коэффициенты теплообмена посредством вычерчивания соответствующей статистической кривой, основанной на большом количестве данных, чтобы сделать минимальным влияние ошибки отдельного измерения. Полученные кривые экстраполируются для определения соответствующих значений на стенке.